ISSN: 0976-3031

Available Online at http://www.recentscientific.com

CODEN: IJRSFP (USA)

International Journal of Recent Scientific Research
Vol. 9, Issue, 1(A), pp. 22913-22918, January, 2018

International Journal of Recent Scientific Research

DOI: 10.24327/IJRSR

Research Article

MD SIMULATION STUDIES OF THE INTER HELICAL INTERACTION FOR TRIMERIC gp41 (N43-L6-CP-IDL) 6HB OF HIV-1 ENVELOPE PROTEIN

Vishnudatt Pandey*., Gargi Tiwari., Vijaya S Mall., Rakesh K Tiwari and Rajendra P Ojha*

Department of Physics, Deen Dayal Upadhyay Gorakhpur University, Gorakhpur, India-273009

DOI: http://dx.doi.org/10.24327/ijrsr.2018.0901.1360

ARTICLE INFO

Article History:

Received 20th October, 2017
Received in revised form 29th November, 2017
Accepted 30th December, 2017
Published online 28th January, 2018

Key Words:

CP-IDL; 6HB; Free Energy Calculations; HIV-1 entry; MD simulations

ABSTRACT

HIV-1 envelope glycoprotein-mediated fusion is managed by the concerted coalescence of the HIV-1 gp41 N- and C-helical regions, which is a product in the formation of 6-helix bundles. These two regions are considered prime targets for peptides and antibodies that inhibit HIV-1 entry. Most of HIV fusion inhibitors against gp41 are peptides derived from the helical C-terminal heptad repeat (CHR) of gp41, including a number of currently experimental drugs and T20 (Enfuvirtide, Fuzeon), the first and only gp41-targeting anti-HIV agent approved by the U.S. FDA. There are so many rational method aimed to attach a rationally designed artificial tail to the C-terminus of HIV-1 fusion inhibitors to increase their antiviral potency. Here we have a crystal structure which report a rationally designed novel HIV-1 fusion inhibitor derived from CHR-derived peptide (Trp628~Gln653, named CP), but with an innovative Ile-Asp-Leu tail (IDL) that dramatically increased the inhibitory activity by up to 100 folds. Crystal structures of artificial fusion peptides N36- and N43-L6-CP-IDL was also available . Although the overall structures of both fusion peptides share the canonical six-helix bundle (6-HB) configuration, their IDL tails adopt two different conformations: a one-turn helix with the N36, and a hook-like structure with the longer N43. Here M. D. simulation was performed to go insight for study of C-terminal tail of Ile-Asp-Leu (IDL).

INTRODUCTION

The acquired immunodeficiency syndrome (AIDS) caused by human immunodeficiency virus (HIV) is still consid-ered as one of the most life-threatening diseases. Due to the gradual increase in new HIV infections, more than 60 million people have been infected with HIV and over 25 million have died from the disease [1]. No efficient vaccines against the virus are currently available. In particular, HIV-1 fusion/entry inhibitors can target early steps of the HIV replication cycle, and they can be used to treat patients who fail to respond to the RTIs and PIs [2]. HIV-1 gp41 is composed of 345 amino acid residues, corresponding to the sequence of 512-856 of the HXB2 gp160 [3] [4].It consists of an ectodomain (residues 512–683), a trans-membrane domain (TM, residues 684–704) and a cytoplasmic domain (CP, residues 705–856). The ectodomain of HIV gp41 contains three important functional regions: the fusion peptide (FP, residues 512–527), the N-terminal heptad repeat (NHR, residues 542–592), and the C-terminal heptad repeat (CHR, residues 623–663) shown in Figure(1) Fusion of the HIV-1 envelope and target cell membranes is initiated by binding of the viral envelope surface subunit gp120 to the cellular CD4, and then to a co-receptor (CCR5 or CXCR4) on the target cell. The available 6 helical bundle structure contains the α-helical NHR and CHR sub domains. Membrane subunit gp41 changes conformation by inserting the FP into the target cell membrane. Three NHR domains form the central trimeric coiled coils that have three hydrophobic grooves, each one containing a deep hdrophobic pocket. Three CHR helices then pack into the grooves on the NHR-trimer in an antiparallel manner to form a six-helix bundle (6-HB) core, which brings the viral and target cell membranes into close proximity for fusion The available 6 helical bundle structure contains the -helical NHR and CHR sub domains. Three CHR helices then pack into the grooves on the NHR-trimer in an antiparallel manner to form a six-helix bundle (6- HB) core, which brings the viral and target cell membranes into close proximity for fusion [5] [6] [7] [8]. The HIV-1 gp41 hydrophobic pocket plays an important role in stabilizing gp41 6-HB core formation and gp41-mediated membrane fusion [9] [10]. Binding of a molecule to the pocket may block HIV-1 fusion with the host cell, suggesting that this pocket is an important target for development of HIV-1 entry

Corresponding author:* **Vishnudatt Pandey
Department of Physics, Deen Dayal Upadhyay Gorakhpur University, Gorakhpur, India-273009

inhibitors. There are so many rational methods to design artificial tail to the C-terminus of HIV-1 fusion inhibitors and increase their antiviral potency. Finally, by introducing an innovative C-terminal tail of Ile-Asp-Leu (IDL), researchers succeeded to increase the anti-HIV potency of a CHR-derived peptide (Trp628 Gln653, named CP,) by more than 100-fold [4]. Interestingly, the crystal structures of CP-IDL in complex with NHR helices at different lengths (N36: Ser546 Leu581, and N43: Val539 Leu581. IDL tail is capable to bear two different conformations: a part of a helix with N36 or a hook-like structure (with N43) recently [4]. for We performed molecular dynamics simulation for N43: Val539 Leu581. IDL and observed that same approaches are possible in the improvement of CHR-derived fusion inhibitors against other viruses.

MATERIAL AND METHODS

Molecular Dynamics Simulations (MD): MD Simulation were performed at the molecular level using the AMBER 14 program with the AMBER ff14SB force field. The crystal structures of gp41 were obtained from the protein data bank (PDB) with pdb identifier 5HFM [4]. Missing hydrogens and other heavy atoms were added by LEaP module of Amber 14. [11] Structure of gp41 complex were solvated in a truncated octahedral box of TIP3P water model that extend to 12 Å of protein boundary in each direction in solute.[12]. An appropriate numbers of ions were added to neutralize the charges of the system. To calculate the non-bonded interactions, the cut-off distance was kept at 12 Å. After proper parameterizations and setup, the resulting system's geometries were minimized (5000 steps for steepest descent and 10000 steps for conjugate gradient) to remove the poor contacts and relax the system. The systems were then gently annealed from 10 to 300 K under canonical ensemble for 50 ps with a weak restraint of 5kcal/mol/Å^2. Subsequently, the systems were maintained for 1 ns of density equilibration under isothermal-isobaric ensemble at target temperature of 300K and the target pressure of 1.0 atm using Langevin-thermostat [13] and Berendsen barostat [14] with collision frequency of 2 ps and pressure relaxation time of 1 ps, with a weak restraint of 1 kcal/mol/Å^2. This 1 ns of density equilibration is not identical with conformational equilibration, but rather a weakly restrained MD in which we slowly relax the system to achieve a uniform density after heating dynamics under periodic boundary conditions. Thereafter, we removed all restraints applied during heating and density dynamics and further equilibrated the systems for ~3 ns to get well settled pressure and temperature for conformational and chemical analysis. This was followed by a productive MD run, for each system, for 100 ns. During all MD simulations, the covalent bonds containing hydrogen were constrained using SHAKE, [15]and particle mesh Ewald (PME) [16] was used to treat long-range electrostatic interactions. We used an integration step of 2 fs during the entire simulations. All MD simulations were performed with GPU version of Amber 14 package [17]. All analysis of trajectories were done using PTRAJ module of Amber 14.

Stability and free energy calculations

The MMGBSA method [18][19] is used for the calculations of thermodynamic parameters and free energy of binding. The principles of these methods are well established [20][21] and have been successfully applied for dengue envelope protein in previous studies [22][23][24]. Here the specific parameters employed in our approach are discussed. The free energy difference of binding is composed of the following terms:

$$\Delta G_{total} = \Delta G_{ele} + \Delta G_{vdw} + \Delta G_{pol} + \Delta G_{nonpol}$$

Here, the first two components in the right hand side represent the electrostatic and van der Waals components of the gas phase molecular mechanics free energy difference, the third term is the electrostatic polar components of the solvation free energy, and the fourth term is the non-polar component of the solvation free energy. All terms are calculated using the standard MMGBSA method implemented in Amber14. The binding free energy among all the three chains of N43 and CP-IDL region was calculated by treating one chain as a ligand and rest two as receptors.

RESULTS AND DISCUSSION

Molecular dynamics simulation was performed to know the intra-domain interactions between different chains which are responsible for conformational rearrangement of the gp 41 of HIV envelope protein. What was effect of CHR based rationally designed artificial tail IDL in stability of NHR-CHR 6HB of gp41 and what was thermodynamics contribution in stability, we performed 150 ns molecular dynamics simulation of N43-L6-CP-IDL terminal of gp41 of HIV envelope protein for the study of their stability for making 6HB formation and energy contribution. To evaluate the convergenceof MD trajectories, the root mean square deviation (RMSD) of the backbone atoms relative to the starting structure during the MD production phase was calculated.

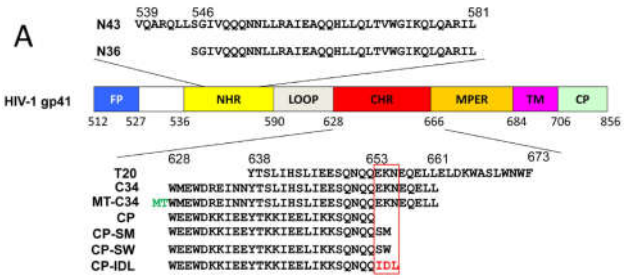

Fig 1 Schematic illustration of HIV-1 gp41 functional regions and NHR- or CHR-derived peptide sequences. The residue numbers of each region correspond to their positions in gp160 of HIV-1HXB2. FP, fusion peptide; CP, cytoplasmic peptide. The MT hook residues in the N terminus of CHR are marked in green. The IDL hook residues in the C terminus are marked in red.

Stability during Simulation

The interaction structures during simulation of gp41 N43-L6-CP-IDL region is shown in figure (2). The RMSD examination from the initial minimized structure for the protein atoms evaluate the reliable stability of the MD trajectory and the difference in the stability of MD simulation the RMSD values of alpha atoms of 5HFM with respect to starting structure over the 150 ns simulation are monitored as shown in Figure(3). Here all the three chains show very low RMSD value with respect to their initial structure.

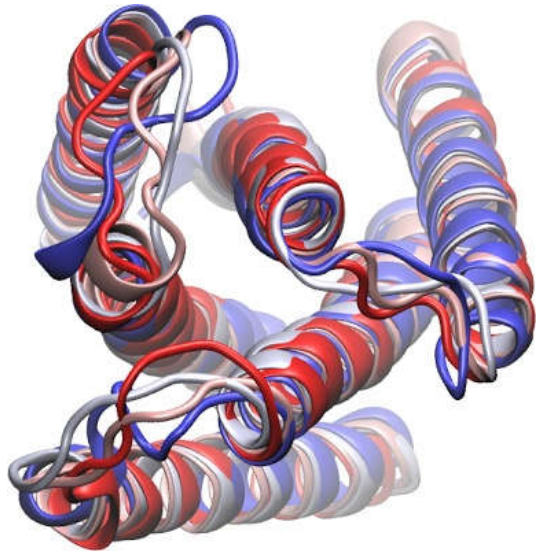

Fig 2 Interaction of chains during simulation

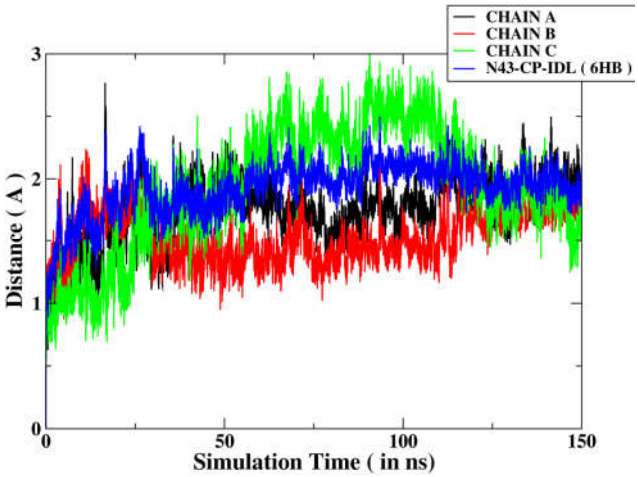

Fig 3 RMSD of all chains A, B and C with N-43,CP-IDL of gp41

The RMSD value for all the three chain and N43-CP-IDL (6HB) are nearly equal to 2.0 angstrom. Chain C is deviated more than chain A and chain B respectively. Thus all the three chains are in equilibrium and reached nearly 1.5 angstrom after 15 ns simulation, indicating good agreement with the x ray crystal structure. The nomenclature for all the three chain in gp 41 trimers are well under stood in Figure(4).

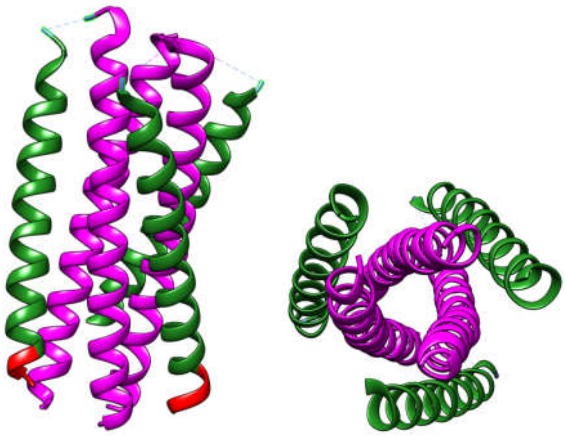

Fig 4 N43-L6-CP-IDL shown in both side view and cross-section view. NHR is colored in purple and C34 is in forest colour. In N36-L6-CP-IDL, CP is in forest and IDL is in red colour.

The RMSD value for 6HB is very high which shows that 6 HB is more deviated field during simulation but the NHR and CHR domains of gp 41 have same RMSD value and the RMSD value is nearly 1 angstrom during whole simulation. The RMSD for CP-IDL (Trp628~Gln653, named CP) chains and IDL (Ile-Asp-Leu)tail chains is shown in figure (5).

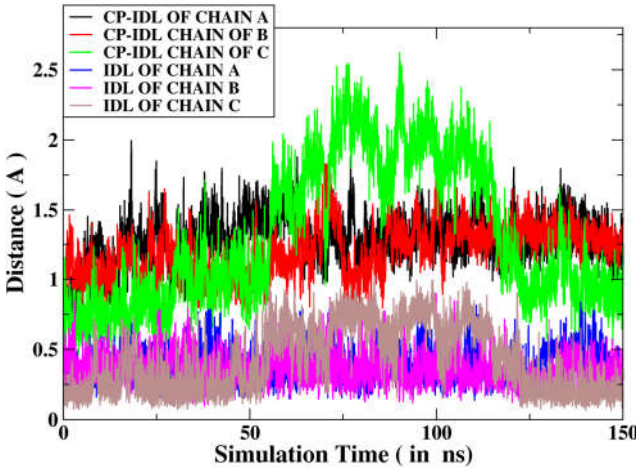

Fig 5 RMSD of CP-IDL and IDL for Chain A,B and C.

Here all the chain of IDL shows very stable and constant RMSD during simulation. RMSD curves for N43 chains with whole 6 HB are also shown in figure (6) whwere all the chains shows again very stable values along with NHR-CHR region. If we Calculate the value of RMSD with N36 Chain then we find that CP-IDL are same as shown in figure (6).

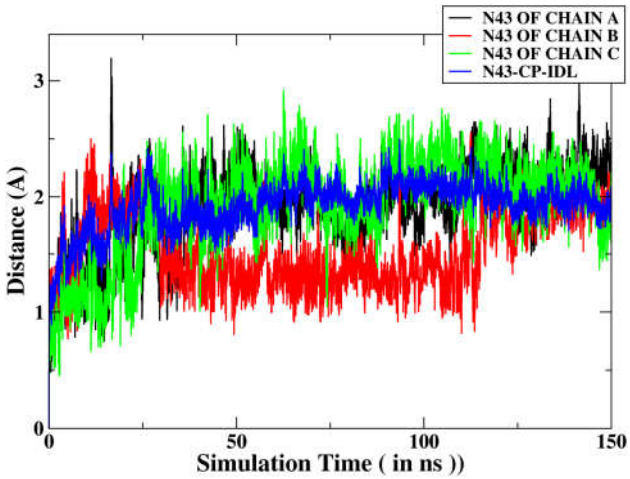

Fig 6 RMSD of N43 for Chain A,B and C and 6HB.

We calculated the solvent accessible surface area (SASA) of each N43 chains to qualify the hydrophobic interactions with CP-IDL and IDL during the entire 150 ns simulations. In figure (7 a) the SASA calculation was given from where we can see that CP-IDL chains shoesnearly 2200 to 2500 angstrom area while in figure (7 b) the SASA Calculation for all the chain are mainly ranges from 250 to 300. However, the interface area between a hook-like IDL tail and an NHR trimer was roughly stable in the range of 250~300 Å2, contributing 12~25% of the interface between CP-IDL and NHR .Interestingly, the total interface area of three IDL tails in the same 6-HB is more stable than individual tails, possessing a contribution of 15~22% .

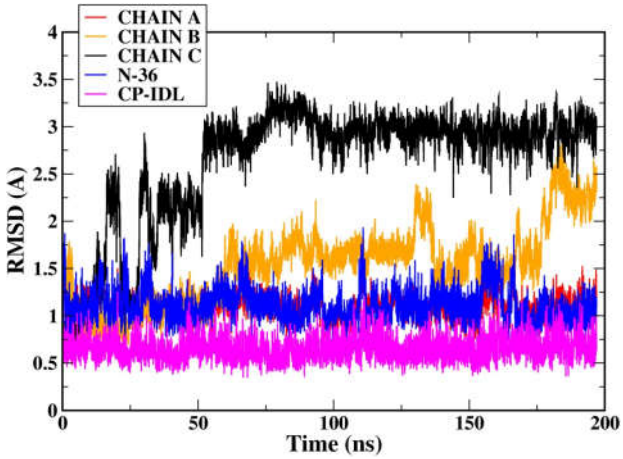

Fig 7 RMSD of N36 for Chain A,B and C and 6HB.

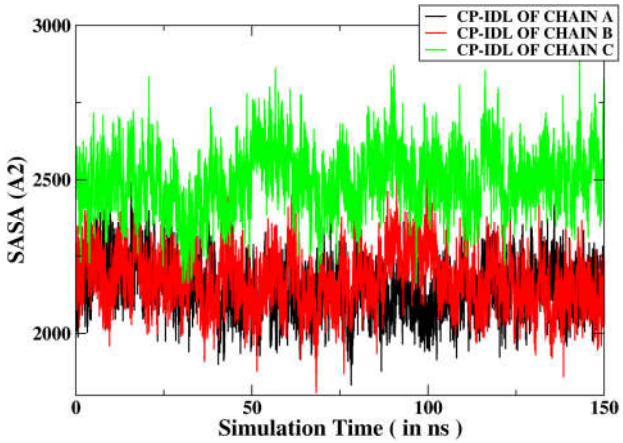

Fig 7 a Solvent accessible surfacearea (SASA) for all chains of CP-IDL during MD simulations.

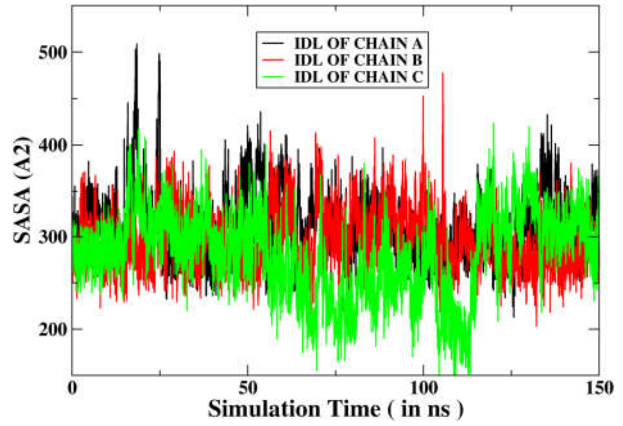

Fig 7 b Solvent accessible surfacearea (SASA) for all chains of IDL during MD simulations.

Inhibitor–residues interaction decomposition

The contribution of each residue to the binding free energy was also evaluated by means of free energy decomposition at the atomic level. This decomposition was for molecular mechanics and solvation energies and not for entropies. The binding energy of each residue pair consists of these terms:

$G_{inhibitor\text{-}residue} = E_{ele} + E_{vdW} + G_{gb} + G_{surf}$

where Eele and EvdW are non-bonded electrostatic interaction and van der Waals energy between the inhibitor and each residue in the gas phase, respectively.

Binding free energy calculation and free energy decomposition

To further evaluate the differences in the binding modes of inner core and to obtain detailed insights into the effect of each component contributed to the in inner core, the binding energies of chain complexes are examined. Binding free energy is calculated using method, in which the entropy calculation is excluded due to high computational cost. We simulated our system till 150 ns and recorded the coordinate every 30 ps. There were a total of 5000 snapshots. For energy computation, we chose the 200 snapshots with interval 1500 steps. Due to the long intervals between each snapshots, they were considered independent and non-correlated. Therefore, due to their ability to represent the whole equilibrium process they could be utilized to calculate the overall binding energy. MMGBSA method were performed to evaluate the general binding activity. Here we took all the chain together and are calculated binding free energy of inner core complex. We calculated binding energy first as a considered IDL chains as a ligands and then CP-IDL as ligand. All the binding energies have been calculated and listed in table (1) understanding the basic mechanism of chain A, chain B and chain C of IDL and CP-IDL.

Table 1 a) The binding affinities for all drugs. All energy values are in kcal mol-1. MMGBSA energy calculations for complex when IDL treated as a ligand.

Differences (Complex - Receptor - Ligand):

Energy Component	Average	Std. Dev.	Std. Err. of Mean
BOND	0.0443	0.0132	0.0093
ANGLE	2.3064	0.0708	0.0500
DIHED	9.0999	0.5480	0.3875
VDWAALS	-17.1918	2.8664	2.0269
EEL	-333.1792	4.2597	3.0120
1-4 VDW	1.0853	0.6266	0.4431
1-4 EEL	37.9297	0.1210	0.0856
EGB	283.2811	6.2481	4.4180
ESURF	-3.3671	0.0267	0.0189
DELTA G gas	-299.9054	5.8880	4.1634
DELTA G solv	279.9141	6.2214	4.3992
DELTA TOTAL	-19.9913	0.3334	0.2358

Table 1 b) MMGBSA energy calculations for complex when CP-IDL treated as a ligand.

Differences (Complex - Receptor - Ligand):

Energy Component	Average	Std. Dev.	Std. Err. of Mean
BOND	0.2686	0.2205	0.1559
ANGLE	4.0254	1.0890	0.7700
DIHED	14.0066	1.0854	0.7675
VDWAALS	-129.9515	7.9719	5.6369
EEL	-226.0602	25.0199	17.6917
1-4 VDW	1.9098	0.3138	0.2219
1-4 EEL	67.7532	0.6277	0.4438
EGB	188.6220	19.2626	13.6207
ESURF	-18.5492	0.5577	0.3944
DELTA G gas	-268.0481	15.8897	11.2357
DELTA G solv	170.0728	18.7049	13.2264
DELTA TOTAL	-97.9753	2.8152	1.9906

The binding energy for all the chains are same .The contribution of each residue to the binding free energy was also evaluated by means of free energy decomposition at the atomic level for different residues with IDL and CP-IDL chains shown in table 2.

Table 2 Energy decomposition per residue for all residues of CP-IDL chains

DELTAS:
Total Energy Decomposition:

Resid 1	Resid 2	Internal	van der Waals	Electrostatic	Polar Solvation	Non-Polar Solv.	TOTAL
ARG 5	LEU 77	0.000 +/- 0.000	-0.799 +/- 0.358	-17.520 +/- 1.464	17.431 +/- 1.492	-0.675 +/- 0.278	-1.563 +/- 0.608
GLN 6	LEU 77	0.000 +/- 0.000	-0.100 +/- 0.017	1.419 +/- 0.366	-1.437 +/- 0.372	-0.002 +/- 0.002	-0.120 +/- 0.013
LEU 8	LEU 77	0.000 +/- 0.000	-0.798 +/- 0.013	-0.062 +/- 0.023	-0.203 +/- 0.001	-0.568 +/- 0.011	-1.631 +/- 0.022
SER 9	LEU 77	0.000 +/- 0.000	0.767 +/- 1.386	-10.121 +/- 0.991	2.864 +/- 0.061	-1.416 +/- 0.099	-7.906 +/- 0.234
VAL 12	ILE 75	0.000 +/- 0.000	-0.949 +/- 0.045	0.567 +/- 0.147	-0.514 +/- 0.133	-0.943 +/- 0.101	-1.839 +/- 0.159
VAL 12	LEU 77	0.000 +/- 0.000	-1.073 +/- 0.099	-1.804 +/- 0.033	1.363 +/- 0.006	-0.810 +/- 0.085	-2.324 +/- 0.157
GLN 15	GLN 74	0.000 +/- 0.000	-0.249 +/- 0.020	0.014 +/- 0.151	0.224 +/- 0.312	-0.116 +/- 0.012	-0.127 +/- 0.130
ASN 16	GLN 74	0.000 +/- 0.000	-0.606 +/- 0.134	-1.468 +/- 2.119	0.096 +/- 0.388	-0.919 +/- 0.089	-2.896 +/- 1.687
LEU 19	ILE 67	0.000 +/- 0.000	-0.853 +/- 0.001	-0.289 +/- 0.013	0.226 +/- 0.004	-0.663 +/- 0.058	-1.581 +/- 0.042
LEU 19	SER 70	0.000 +/- 0.000	-0.865 +/- 0.115	-0.126 +/- 0.009	0.219 +/- 0.012	-0.716 +/- 0.059	-1.487 +/- 0.060
LEU 19	GLN 71	0.000 +/- 0.000	-0.711 +/- 0.042	-0.101 +/- 0.035	0.284 +/- 0.025	-0.739 +/- 0.033	-1.266 +/- 0.019
LEU 19	GLN 74	0.000 +/- 0.000	-0.656 +/- 0.040	-0.126 +/- 0.493	-0.009 +/- 0.286	-0.501 +/- 0.052	-1.292 +/- 0.115
ILE 22	ILE 67	0.000 +/- 0.000	-0.653 +/- 0.011	-0.079 +/- 0.004	0.098 +/- 0.011	-0.581 +/- 0.059	-1.215 +/- 0.078
GLU 23	ILE 67	0.000 +/- 0.000	-0.631 +/- 0.034	-0.528 +/- 0.188	0.504 +/- 0.184	-0.575 +/- 0.041	-1.230 +/- 0.070
GLN 26	ILE 63	0.000 +/- 0.000	-0.931 +/- 0.085	-0.025 +/- 0.092	0.362 +/- 0.072	-0.797 +/- 0.008	-1.391 +/- 0.058
GLN 26	GLU 64	0.000 +/- 0.000	-0.572 +/- 0.112	1.298 +/- 0.262	-1.663 +/- 0.056	-0.397 +/- 0.047	-1.334 +/- 0.365
GLN 30	THR 60	0.000 +/- 0.000	-0.421 +/- 0.047	-2.139 +/- 0.433	0.318 +/- 0.278	-0.785 +/- 0.090	-3.027 +/- 0.753
VAL 33	TRP 52	0.000 +/- 0.000	-0.665 +/- 0.055	-0.203 +/- 0.017	0.162 +/- 0.005	-0.502 +/- 0.009	-1.208 +/- 0.024
VAL 33	ILE 56	0.000 +/- 0.000	-0.772 +/- 0.037	-0.095 +/- 0.025	0.111 +/- 0.025	-0.806 +/- 0.054	-1.562 +/- 0.09
ILE 36	TRP 52	0.000 +/- 0.000	-0.947 +/- 0.169	0.092 +/- 0.004	-0.240 +/- 0.021	-0.796 +/- 0.054	-1.890 +/- 0.241
LYS 37	ARG 46	0.000 +/- 0.000	-1.803 +/- 0.315	27.034 +/- 0.358	-26.121 +/- 0.025	-1.339 +/- 0.104	-2.229 +/- 0.036
LYS 37	ASP 53	0.000 +/- 0.000	-0.372 +/- 0.252	-29.058 +/- 5.461	28.022 +/- 4.588	-0.233 +/- 0.212	-1.641 +/- 1.336
GLN 40	ARG 46	0.000 +/- 0.000	-0.957 +/- 0.461	-8.523 +/- 1.538	2.606 +/- 0.392	-1.139 +/- 0.027	-8.013 +/- 1.442
GLN 40	TRP 49	0.000 +/- 0.000	-1.688 +/- 0.503	-1.272 +/- 0.365	-0.076 +/- 0.274	-1.551 +/- 0.078	-4.587 +/- 0.214
GLN 40	TRP 52	0.000 +/- 0.000	-0.877 +/- 0.258	-0.788 +/- 0.356	0.296 +/- 0.073	-0.484 +/- 0.140	-1.852 +/- 0.828
ALA 41	ARG 46	0.000 +/- 0.000	-0.691 +/- 0.102	0.523 +/- 0.115	-0.799 +/- 0.044	-0.538 +/- 0.065	-1.505 +/- 0.238
ILE 43	GLY 44	0.000 +/- 0.000	-0.604 +/- 0.082	-26.043 +/- 0.149	-0.206 +/- 0.266	-0.934 +/- 0.001	-27.786 +/- 0.33
GLY 44	ILE 43	0.000 +/- 0.000	-0.604 +/- 0.082	-26.043 +/- 0.149	-0.206 +/- 0.266	-0.930 +/- 0.085	-27.783 +/- 0.249
ARG 46	LYS 37	0.000 +/- 0.000	-1.803 +/- 0.315	27.034 +/- 0.358	-26.121 +/- 0.025	-1.336 +/- 0.094	-2.226 +/- 0.026
ARG 46	GLN 38	0.000 +/- 0.000	-0.116 +/- 0.033	-0.191 +/- 0.991	0.061 +/- 0.998	-0.007 +/- 0.007	-0.253 +/- 0.047
ARG 46	GLN 40	0.000 +/- 0.000	-0.957 +/- 0.461	-8.523 +/- 1.538	2.606 +/- 0.392	-1.158 +/- 0.021	-8.032 +/- 1.448
ARG 46	ALA 41	0.000 +/- 0.000	-0.691 +/- 0.102	0.523 +/- 0.115	-0.799 +/- 0.044	-0.535 +/- 0.065	-1.502 +/- 0.238
ARG 46	ASP 53	0.000 +/- 0.000	0.000 +/- 0.000	0.000 +/- 0.000	-2.819 +/- 0.785	0.058 +/- 0.052	-2.760 +/- 0.733
GLY 47	ARG 119	0.000 +/- 0.000	0.734 +/- 0.913	-5.913 +/- 4.813	2.177 +/- 1.066	-0.313 +/- 0.208	-3.315 +/- 3.042
GLY 48	ARG 119	0.000 +/- 0.000	-0.521 +/- 0.024	-1.819 +/- 0.224	1.722 +/- 0.149	-0.466 +/- 0.092	-1.083 +/- 0.191
TRP 49	GLN 40	0.000 +/- 0.000	-1.688 +/- 0.503	-1.272 +/- 0.365	-0.076 +/- 0.274	-1.470 +/- 0.055	-4.506 +/- 0.191
TRP 49	GLN 115	0.000 +/- 0.000	-1.002 +/- 0.290	-0.204 +/- 0.413	-0.237 +/- 0.229	-0.850 +/- 0.003	-2.293 +/- 0.103
TRP 49	LEU 116	0.000 +/- 0.000	-0.610 +/- 0.086	-0.076 +/- 0.002	0.055 +/- 0.022	-0.612 +/- 0.151	-1.243 +/- 0.045
TRP 49	ARG 119	0.000 +/- 0.000	-1.134 +/- 0.044	-0.894 +/- 0.148	-0.277 +/- 0.783	-0.920 +/- 0.122	-3.225 +/- 0.801
TRP 52	VAL 33	0.000 +/- 0.000	-0.665 +/- 0.055	-0.203 +/- 0.017	0.162 +/- 0.005	-0.464 +/- 0.002	-1.170 +/- 0.031
TRP 52	ILE 36	0.000 +/- 0.000	-0.947 +/- 0.169	0.092 +/- 0.004	-0.240 +/- 0.021	-0.728 +/- 0.065	-1.822 +/- 0.252
TRP 52	GLN 40	0.000 +/- 0.000	-0.877 +/- 0.258	-0.788 +/- 0.356	0.296 +/- 0.073	-0.475 +/- 0.125	-1.843 +/- 0.813
TRP 52	LEU 108	0.000 +/- 0.000	-1.304 +/- 0.422	-2.459 +/- 0.428	0.713 +/- 0.060	-1.183 +/- 0.058	-4.233 +/- 0.731
TRP 52	GLY 112	0.000 +/- 0.000	-0.702 +/- 0.069	0.467 +/- 0.175	-0.401 +/- 0.036	-0.513 +/- 0.082	-1.149 +/- 0.013
ASP 53	LYS 37	0.000 +/- 0.000	-0.372 +/- 0.252	-29.058 +/- 5.461	28.022 +/- 4.588	-0.224 +/- 0.204	-1.632 +/- 1.328
ASP 53	ARG 46	0.000 +/- 0.000	0.000 +/- 0.000	0.000 +/- 0.000	-2.819 +/- 0.785	0.057 +/- 0.037	-2.761 +/- 0.748
LYS 55	LEU 108	0.000 +/- 0.000	-0.424 +/- 0.192	0.621 +/- 0.113	-0.525 +/- 0.118	-0.726 +/- 0.047	-1.055 +/- 0.150
ILE 56	VAL 33	0.000 +/- 0.000	-0.772 +/- 0.037	-0.095 +/- 0.025	0.111 +/- 0.025	-0.815 +/- 0.047	-1.571 +/- 0.084

CONCLUSIONS

The Binding complex of gp 41 N43-CP-IDL 6HB core structures is simulated. Free energy analysis of protein chain complex for IDL chains and CP-IDL chains treating one chain as a ligand and other as a receptor and whole as a complex, was used to identify the responsible residue for binding in terms of free energy. Our simulation shows that ILE, ARG, TRP, GLU, PRO, SER, LYS are most responsible residue for bringing an inner coil helix together as their decomposition energies are very high. In spite of that electrostatic interaction plays an important role in determining the affinities of the chain binding and stabilizes N43-CP-IDL chains . Here IDL tails also enhance the binding affinity of whole complex.

Acknowledgment

The Computational resources were provided by BRAF, CDAC, Pune and the partial computational work is done at Supercomputing facility for bioinformatics and computational biology, Indian Institute of Technology, New Delhi, India, their support is gratefully acknowledged. We wish to earnestly express our gratitude for Prof. B. Jayaram, coordinator SCFbio, Indian Institute of Technology, New Delhi (IITD) to facilitate the supercomputer access.

References

1. Cohen MS, Hellmann N, Levy JA, DeCock K, Lange J. The spread, treatment, and prevention of HIV-1: evolution of a global pandemic. *J Clin Invest*. 2008, 118, 12441254
2. Kilby, J.M. Hopkins, S. Venetta, T.M. DiMassimo, B. Cloud, G.A. Lee,J.Y. Alldredge, L. Hunter, E.; Lambert, D.; Bolognesi, D., *Nat. Med*. 1998, 4, 13021307
3. Kuiken C L, *et. al* , Nat Lab UR 01-3860
4. Yun Z, Shan S, Lili Q, Qian W, Lei S, Zhenxuan M, Jianchao T S, Jiang L, Lu S Y, Rongguang Z, srep, 2016,6:31983 DOI: 10.1038/srep31983
5. Allan, J.S.; Coligan, J.E.; Barin, F.; McLane, M.F.; Sodroski, J.G.; Rosen,C.A.; Haseltine, W.A.; Lee, T.H.; Essex, M. *Science* 1985, 228, 10911094
6. Moore, J.P.; Jameson, B.A.; Weiss, R.A.; Sattentau, Q.J. Bentz, J., Ed., CRC Press: Boca Raton, FL, USA,1993, 233289
7. Berger, E.A SupplS3S16, 1997, 11
8. Chan, D.C.; Kim, P.S. Cell 1998, 93, 681-684
9. Chutkowski D C, Kim, P.S. Proc. Natl. Acad. Sci. USA,

1998, 95, 1561315617
10. Ji, H.; Shu, W.; Burling, T.; Jiang, S.; Lu, M. *J. Virol.* 1999 73, 85788586
11. AmberTools12 Reference Manual
12. KEMIN TAN*, JIN-HUAN LIU*, JIA-HUAI WANG*†‡, Steven Shen§, And MIN LU 13, 3 435-450Proc. *Natl. Acad*. Sci. USA Vol. 94, pp. 12303-12308, November 1997
13. Izaguirre, J. A.; Catarello, D. P.; Wozniak, J. M.; Skeel, R. D. *J. Chem. Phys.*2001, 114, 2090-2098.
14. Berendsen, H. J. C.; Postma, J. P. M.; van Gunsteren, W. F.; DiNola, A.; Haak, J. R. *J. Chem. Phys*. 1984, *81*, 3684−3690.
15. Ryckaert, J.-P.; Ciccotti, G.; Berendsen, H. J. C. *J. Comput. Phys*. 1977, *23*, 327-341.
16. Darden, T.; York, D.; Pedersen, L. *J. Chem. Phys*. 1993, *98*, 1008910092.
17. Salomon-Ferrer, R.; Götz, A. W.; Poole, D.; Le Grand, S.; Walker, R. C. J. *Chem. Theor. Comput.* 2013, *9*, 3878-3888.
18. Gohlke H, Case DA. Converging free energy estimates: MM-PB (GB) SA studies on the Protein-Protein Complex Ras-Raf. *J Comput Chem*. 2003. 25:238-250.
19. Fogolari F, Brigo A, Molinari H. Protocols for MM/PBSA molecular dynamics simulations of proteins. *Biophys* 2003. J. 85:159-166.
20. Grochowaski P, Trylska J. Continuum molecular electrostatics, salt effects, and counterion binding- a review of the poisson-boltzmann theory and its modifications. *Biopolymers*. 2007. 89:93-113.
21. Tsui V, Case DA. Theory and application of generalized born solvation model in macromolecular simulations. *Biopolymers*. 2001. 56:271-291.
22. Dubey KD, Chaubey AK, Ojha RP. Role of pH on dimeric interactions for DENV envelope protein: An insight from molecular dynamics study. *Biochim Biophys Acta*. 2011, 1814: 1796-1801.
23. Dubey KD, Chaubey AK, Ojha RP. Stability of trimeric DENV envelope protein at low and neutral pH: an insight from MD study. *Biochim Biophys Acta* 2013. 1834: 53-64.
24. Pandey V, Tiwari G, Ojha R P *International Journal of Pure and Applied Physics* 2017.

How to cite this article:

Vishnudatt Pandey *et al*.2018, MD Simulation Studies of The Inter Helical Interaction For Trimeric gp41 (N43-L6-CP-IDL) 6HB of HIV-1 Envelope Protein. *Int J Recent Sci Res.* 9(1), pp. 22913-22918.
DOI: http://dx.doi.org/10.24327/ijrsr.2018.0901.1360

****